Tetrahedron Letters 52 (2011) 4030–4035

Contents lists available at ScienceDirect

Tetrahedron Letters

journal homepage: www.elsevier.com/locate/tetlet

Informative secondary chiroptics in binary molecular organogel systems for donor–acceptor energy transfer

Koji Miyamoto [a], Hirokuni Jintoku [a], Tsuyoshi Sawada [a], Makoto Takafuji [a], Takashi Sagawa [b], Hirotaka Ihara [a,c,*]

[a] Department of Applied Chemistry and Biochemistry, Kumamoto University, Kumamoto 860-8555, Japan
[b] Institute of Advanced Energy, Kyoto University, Gokasho, Uji Kyoto 611-0011, Japan
[c] Kumamoto Institute for Photo-Electro Organics (Phenics), Kumamoto 862-0901, Japan

ARTICLE INFO

Article history:
Received 15 April 2011
Revised 22 May 2011
Accepted 27 May 2011
Available online 2 June 2011

Keywords:
Organogel
Energy transfer
FRET
Chiroptics
Excimer

ABSTRACT

Pyrene-doped L-glutamide-based lipidic derivatives with different alkyl lengths (***C*$_n$*-g-Pyr**; $n = 4$, 8 and 12) were newly synthesized. All of the ***C*$_n$*-g-Pyr** dissolved and showed thermotopically and lyotropically-induced excimer formations accompanied by induction of the positive Cotton effect in their CD spectra, indicating chirally ordered stacking. However, when ***C*$_4$*-g-Pyr** and ***C*$_{12}$*-g-Pyr** were mixed in a certain molar ratio, an unusual CD pattern from positive to negative ones was observed. In this study, energy transfer efficiency was investigated in a binary system of ***C*$_n$*-g-Pyr** with ***C*$_{12}$*-g-TPP**. The results revealed that simple modification of the alkyl length of ***C*$_n$*-g-Pyr** enables enhancement of the energy transfer efficiency with ***C*$_{12}$*-g-TPP**.

One-dimensionally nano-assembled materials have become attractive as molecular electronic devices for mimicking natural photosynthesis[1] in terms of light-harvesting and energy migration[2] when molecular donors and accepters can be integrated into their nanostructures. There are several advantages to the use of these materials over rigid π-conjugated polymer systems including good dispersity, diverseness of chemical tuning and supramolecular functionalization. Conversely, chiral molecules such as amino acids and sugars comprise some of the most useful base materials for one-dimensional fabrication of nanoscale suprastructures.[3] For example, a polymer of amino acids folds spontaneously into one-dimensional rigid structures such as α-helix and 3_1-helix.[4] Furthermore, amino acid-derived amphiphilic and lipophilic molecules often create nanoscale helical, tubular and fibrillar aggregates through molecular ordering in aqueous[5,6] and organic media.[7–9] The similarities between these systems are due to peptide bonds working as the main driving force for the creation of suprastructures with unique chiral signals in their aggregation morphology and chiroptical properties.

In this study, we investigated chiroptical information in amino acid-derived donors and acceptors as model compounds expected to be used in molecular electronic devices. Specifically, we attempted to develop a method enabling the use of a chiroptical signal as an indicator for monitoring, controlling and optimizing the molecular ordering state in a donor–accepter energy transfer system. To accomplish this, we selected L-glutamic acid-based self-assembling tool (***g***)[6–8] and newly synthesized ***g***-functionalized pyrene derivatives with different alkyl lengths as lipophilic moieties[10,11] (***C*$_n$*-g-Pyr**; $n = 4$, 8 and 12) (Scheme 1). We found that simple modification of the alkyl length induced drastic chiroptical changes in their aggregation states and enabled enhancement of the energy transfer efficiency with a porphyrin derivative in a donor–acceptor binary assembled system.

The solubility (dispersity) of ***C*$_n$*-g-Pyr** was evaluated in a 1 mM dispersion. As summarized in Table 1, all ***C*$_n$*-g-Pyr** showed good and wide solubility in various organic solvents at 60 °C, with the exception of *n*-hexane. Conversely, apparent mass gelation behaviours were observed in some organic solvents such as benzene, toluene and cyclohexane at 10 °C. This phenomenon can be classified into "low-molecular mass gelation" or "molecular gelation".[13] TEM observations showed that well-developed nano-fibrillar aggregates were mainly included in the cast film with ***C*$_n$*-g-Pyr** (Fig. S1), which indicated that low-molecular mass gelation can be induced through three-dimensional network formation with fibrillar aggregates.

The finding that N^2,N^3-dialkyl L-glutamide moieties with shorter alkyl groups (***C*$_4$*-g**) have similar organogelation ability to a ***C*$_{12}$*-g**

* Corresponding author. Tel./fax: +81 96 342 3661.
E-mail address: ihara@kumamoto-u.ac.jp (H. Ihara).

0040-4039/$ - see front matter © 2011 Elsevier Ltd. All rights reserved.
doi:10.1016/j.tetlet.2011.05.131

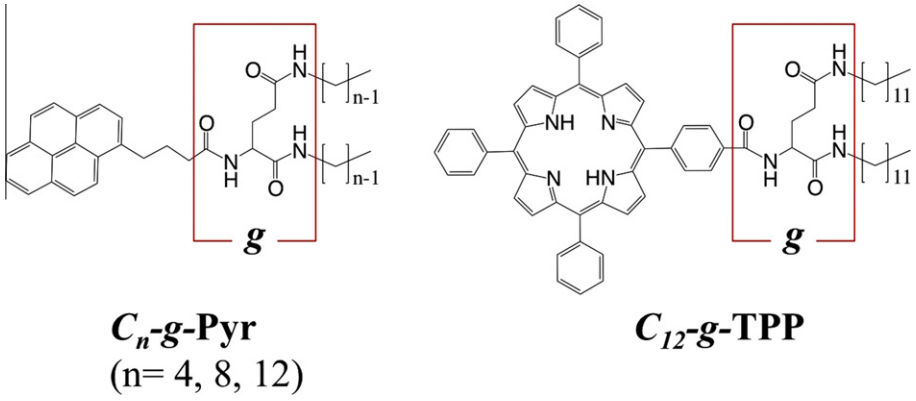

Scheme 1.

Table 1
Solubility of ***C*$_n$-*g*-Pyr** in various organic solvents at 10 and 60 °C

Solvents	ε_r[12]	10 °C			60 °C		
		***C*$_4$-*g*-Pyr**	***C*$_8$-*g*-Pyr**	***C*$_{12}$-*g*-Pyr**	***C*$_4$-*g*-Pyr**	***C*$_8$-*g*-Pyr**	***C*$_{12}$-*g*-Pyr**
n-Hexane	1.88	I	I	I	I	I	I
Cyclohexane	2.02	G	G	G	S	S	S
Benzene	2.27	G	G	G	S	S	S
Toluene	2.38	G	G	G	S	S	S
Chloroform	4.81	S	S	S	S	S	S
Ethyl acetate	6.02	G	G	G	S	S	S
THF	7.58	S	S	S	S	S	S
Acetone	20.5	S	S	P	S	S	S
Ethanol	24.5	S	S	P	S	S	S
Methanol	32.6	S	S	P	S	S	S
Acetonitrile	35.9	P	P	P	S	S	S

Concentration: 1.0 mM, S: solution, I: insoluble, P: precipitation, G: gelation.

moieties is important because it indicates that any long-chain alkyl group can work as a non-conductive moiety when used in a semiconducting organic thin film; thus, a shorter alkyl length such as a ***C*$_4$** group would be more desirable for this purpose. In addition, this finding suggested that the ***g*** moiety is essential for gelation in this system, while the alkyl length affects the solubility or lipophilicity.

The aggregation states of ***C*$_n$-*g*-Pyr** in organic media can be estimated by their chiroptical properties, which are determined by CD and UV spectroscopy because a pyrene moiety is attached to a ***g*** unit with a chiral centre. When ***C*$_n$-*g*-Pyr** was dissolved at 0.25 mM in chloroform the UV spectrum showed a normal pattern with λ_{max}s at 345, 329, and 316 nm, which were assigned to the absorption bands based on a pyrene moiety. Moreover, no specific Cotton effect was observed in the CD spectrum, with the molar ellipticity ($[\theta]_{max}$) around the absorption band of the pyrene moiety being around 1×10^3 deg cm^{-2} dmol^{-1} at temperatures between 10 and 60 °C. Conversely, the use of benzene, which has been identified as an assembling solvent, led to remarkable spectral changes in both the UV and CD spectra while the concentration of measurement was less than the critical gelation concentration (cgc: 0.30 mM in benzene). As shown in Figure 1c, the UV spectra of ***C*$_{12}$-*g*-Pyr** benzene solution showed remarkably reduced absorbance at 345, 329, and 316 nm when the temperature decreased from 60 to 10 °C. Furthermore, this UV spectral change was accompanied by the appearance of a shoulder around 355 nm. In CD spectra, induction of a positive Cotton effect showing R-chirality was indicated with extremely large ellipticity around the shoulder absorption at 10 °C (Fig. 1f). This is understandable based on the induction of secondary chirality[14,15] in response to intermolecular chiral stacking of the pyrene moiety. The detailed CD patterns of ***C*$_4$-*g*-Pyr** and ***C*$_8$-*g*-Pyr** showed slightly different λ_{max} and intensity values at $[\theta]_{max}$. However, similar behaviours could be confirmed in other assembling solvents, such as toluene and ethyl acetate. These findings suggest that all ***C*$_n$-*g*-Pyr** can form chirally ordered secondary structures in an assembling solvent.

An unusual chirality change was observed in binary systems containing the proper combination of ***C*$_4$-*g*-Pyr** and ***C*$_{12}$-*g*-Pyr**. As shown in Figure 2a, a 2-to-1 mixed system of ***C*$_4$-*g*-Pyr** and ***C*$_{12}$-*g*-Pyr** in benzene provided a strong and negative Cotton effect (indicating S-chirality), which was opposite to the signal produced by their single component systems (indicating R-chirality). The remarkable changes were not observed in the cases of ***C*$_{12}$-*g*-Pyr**/***C*$_8$-*g*-Pyr** and ***C*$_8$-*g*-Pyr**/***C*$_4$-*g*-Pyr**. A detailed investigation of this phenomenon revealed several important characteristics. First, $[\theta]_{max}$ in the 2-to-1 binary system was observed at 362 nm, which is slightly red-shifted from its location at 358 and 355 nm in the single component systems of ***C*$_4$-** and ***C*$_{12}$-*g*-Pyr**, respectively. These findings indicated that *J*-type (head-to-tail) orientation (Fig. S2)[10,16] among the pyrene moieties can be promoted by mixing. Second, the chirality inversion in the binary system could only be observed in the narrow condition of a 2:1 mixing ratio of ***C*$_4$-** and ***C*$_{12}$-*g*-Pyr** (Fig. 2b). Third, the 2:1 binary system showed a temperature-dependent transition in the CD intensity that was similar to the system composed of ***C*$_{12}$-*g*-Pyr** alone, while no significant transition was observed in ***C*$_4$-*g*-Pyr** alone (Fig. 3). These findings demonstrate that ***C*$_4$-*g*-Pyr** is compatible with ***C*$_{12}$-*g*-Pyr** in mixed systems and that phase transition behaviour is directly influenced by the components of ***C*$_{12}$-*g*-Pyr**.

Donor–accepter systems have attracted considerable attention as energy transfer models. These can be roughly classified into covalent[17] and non-covalent[18] systems; therefore, the present study can contribute to their use as non-covalent systems when

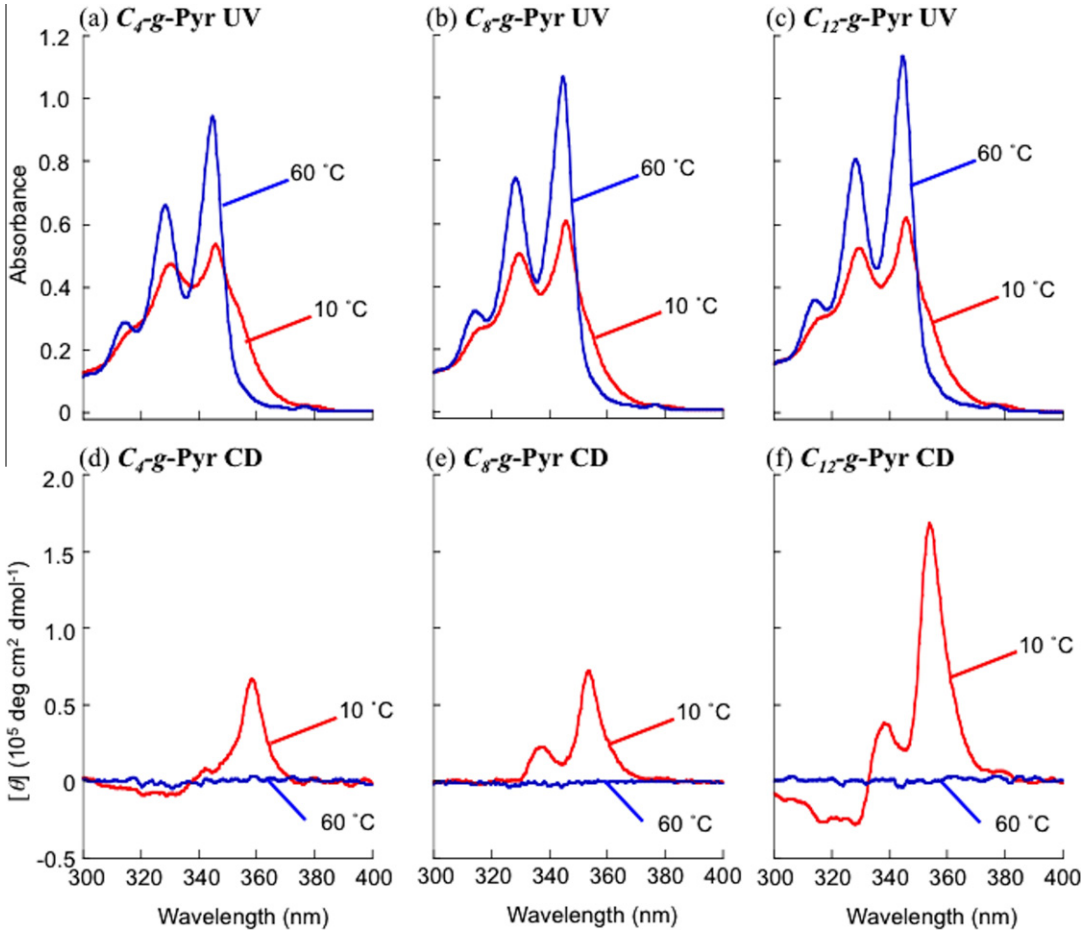

Figure 1. Temperature-dependent UV (a–c) and CD (d–f) spectral changes of ***C*$_n$*-g*-Pyr** (0.25 mM) in benzene at 10 °C (red) and 60 °C (blue).

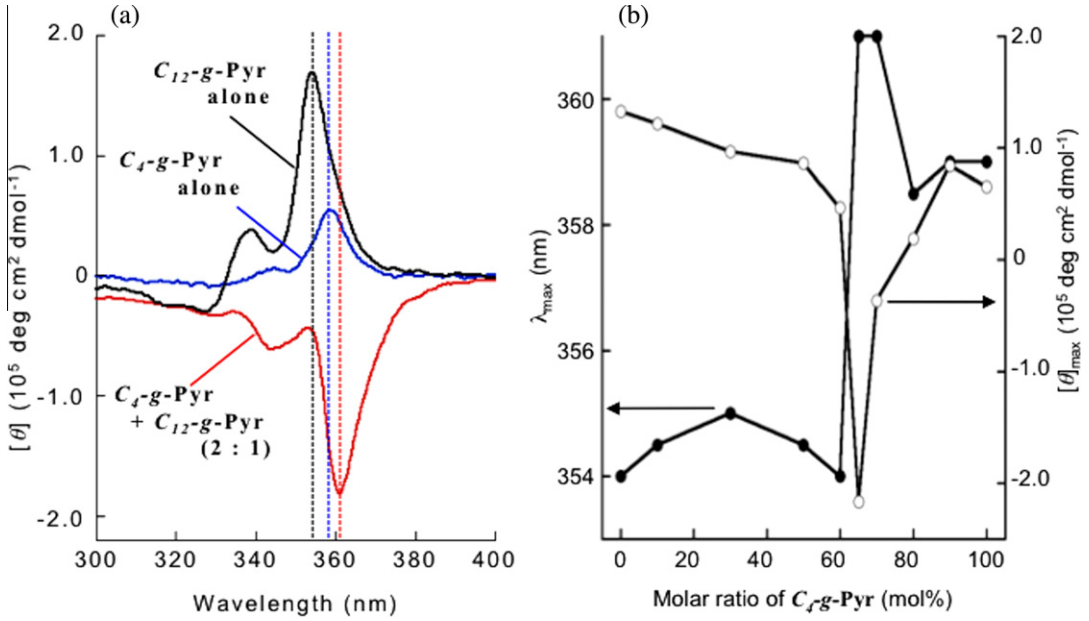

Figure 2. CD spectra of ***C*$_4$*-g*-Pyr** (blue), ***C*$_{12}$*-g*-Pyr** (black) and a 2-to-1 mixture of ***C*$_4$*-g*-Pyr** and ***C*$_{12}$*-g*-Pyr** (red) in benzene at 10 °C. The total concentrations of pyrene were adjusted as 0.25 mM. (b) Dependencies of the molar ratio of ***C*$_4$*-g*-Pyr** on $[\theta]_{max}$ (open circles) and λ_{max} (solid circle) in the binary system of ***C*$_4$*-g*-Pyr** and ***C*$_{12}$*-g*-Pyr** in benzene at 10 °C.

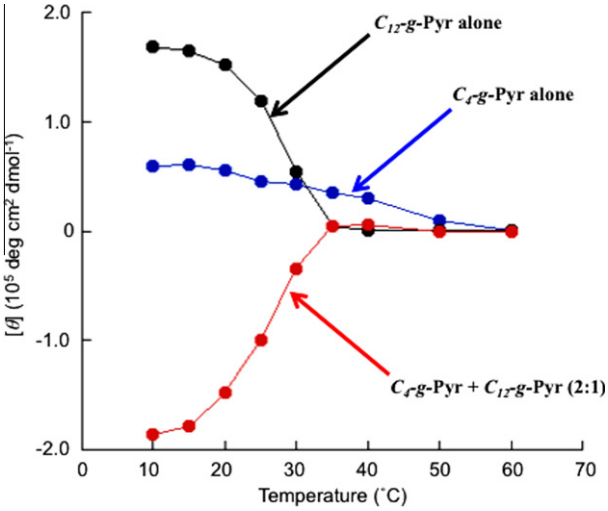

Figure 3. Temperature dependencies of $[\theta]_{\lambda\mu\alpha\xi}$ values of C_n-g-Pyr (n = 4 and 12) and mixture of C_4-g-Pyr and C_{12}-g-Pyr (2:1). Concentrations are 0.25 mM.

an acceptor porphyrin derivative is assembled with C_{12}-g-Pyr as an donor. In this study, C_{12}-g-TPP[19] containing a tetraphenylporphyrin moiety as a donor was selected based on its compatibility with C_n-g-Pyr. Conversely, we found that the molecular ordering states of C_n-g-Pyr could be controlled by choosing the alkyl length in the binary system. These findings encouraged us to investigate the effects of the alkyl length, even in a donor–accepter binary system. Therefore, we investigated the efficiency of energy transfer from C_4-g-Pyr or C_{12}-g-Pyr excimers to C_{12}-g-TPP in this study.

The fluorescence study to investigate the energy transfer was conducted using a cyclohexane–THF mixed system instead of benzene based on the energy transfer efficiency. As shown in Figure 4c, C_{12}-g-Pyr exhibited lyotropically-induced excimeric emission through excitation at 350 nm, which is on the absorption band of the aggregated pyrene. A characteristic fluorescence spectrum (λ_{max}, 445 nm) assigned by an excimer was observed at concentrations above 15 μM in cyclohexane–THF (15:1) mixed systems at 10 °C. On the other hand, the fluorescence spectra at concentrations below 5 μM were similar to those observed in chloroform, indicating it was an excimeric emission with λ_{max} values of 380, 398 and 418 nm. Similar results were obtained for C_4-g-Pyr (Fig. 4a) and C_8-g-Pyr (Fig. 4b), although the fluorescence intensity differed. Excimer formation is an important functionality of C_n-g-Pyr because efficient crossover between an emission band of a monomeric pyrene and an absorption band of a tetraphenylporphyrin derivative as a donor component is expected as a possible pathway to a Förster resonance energy transfer (FRET) system.[20] Indeed, the excimeric emission band of C_n-g-Pyr overlapped with not only the Soret absorption band, but also the Q_α and Q_β bands of tetraphenylporphyrin (Fig. S3).

Energy transfer was monitored and evaluated using the emission intensity at 650 nm based on the Q band of a porphyrin moiety. As shown in Figure 5a, when *g*-free **TPP** (without a *g* unit) was excited at 350 nm in the absence and presence of C_4-g-Pyr, the emission intensity decreased remarkably in the presence of C_4-g-Pyr. These findings can be explained by the fact that the excitation energy is partially consumed by absorption at the aggregated C_4-g-Pyr, but that no significant energy transfer from the C_4-g-Pyr excimer to **TPP** occurs. Conversely, when the *g*-functionalized **TPP** was replaced instead of *g*-free **TPP**, distinct emission enhancement was observed as shown in Figure 5b and c. The combination of C_{12}-g-TPP with C_4-g-Pyr showed a remarkably higher increase than that with C_{12}-g-Pyr. Similar behaviours were observed in cyclohexane/chloroform system as same as in cyclohexane/THF system. In addition, no similar increase in the Q band emission was observed at 60 °C or in chloroform at 10 °C, promoting an ordered-to-disordered transition. These results also indicate that efficient energy transfer can only occur in their aggregated ordered states, and that these are enhanced by the proper adjustment of alkyl chains of the C_n-g derivatives.

In conclusion, we described the effect of alkyl length in L-glutamide-based lipidic compounds with a pyrene moiety (C_n-g-Pyr; n = 4, 8 and 12) on the chiral aggregation state and energy transfer efficiency. C_n-g-Pyr with shorter alkyl chains (e.g. n = 4) were found to have sufficient organogelation ability through nano-fibrillar aggregation. This aggregation was accompanied by the excimer formation and secondary chirality induction based on the molecular orientation. This is an advantageous property because any long chain alkyl group can work as a non-conductive moiety when used in a semiconducting organic thin film. However, when the chiroptical signals were investigated in a binary system of C_n-g-Pyr with different alkyl lengths, a proper combination provided a drastic change in the CD patterns such as a positive-to-negative transition. The results of the present study also revealed that a binary system composed of C_4-g-Pyr and

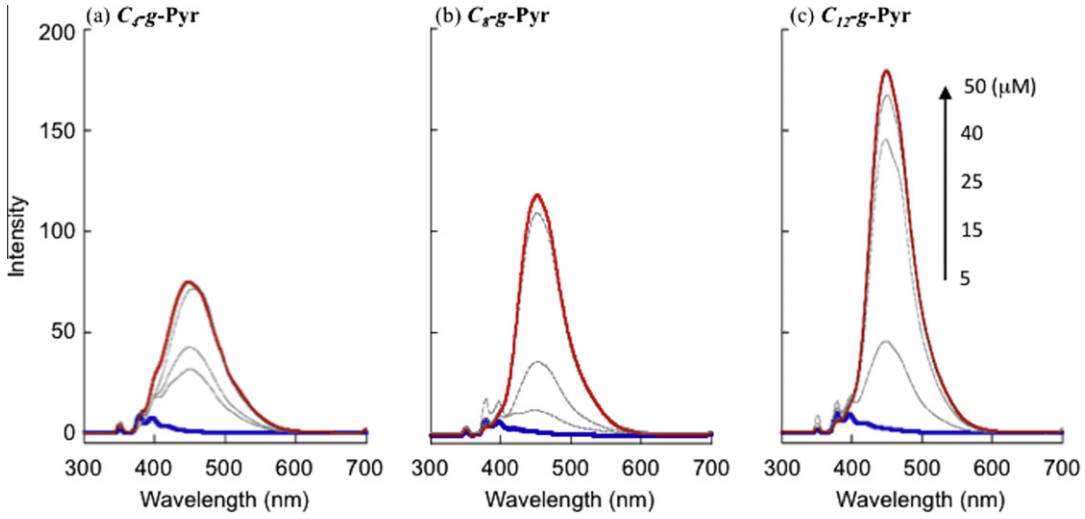

Figure 4. Concentration-dependent excimer emission of C_n-g-Pyr (n = 4 (a), 8 (b) and 12 (c)) in cyclohexane-THF (15:1) at 10 °C. Excitation wavelength: 350 nm.

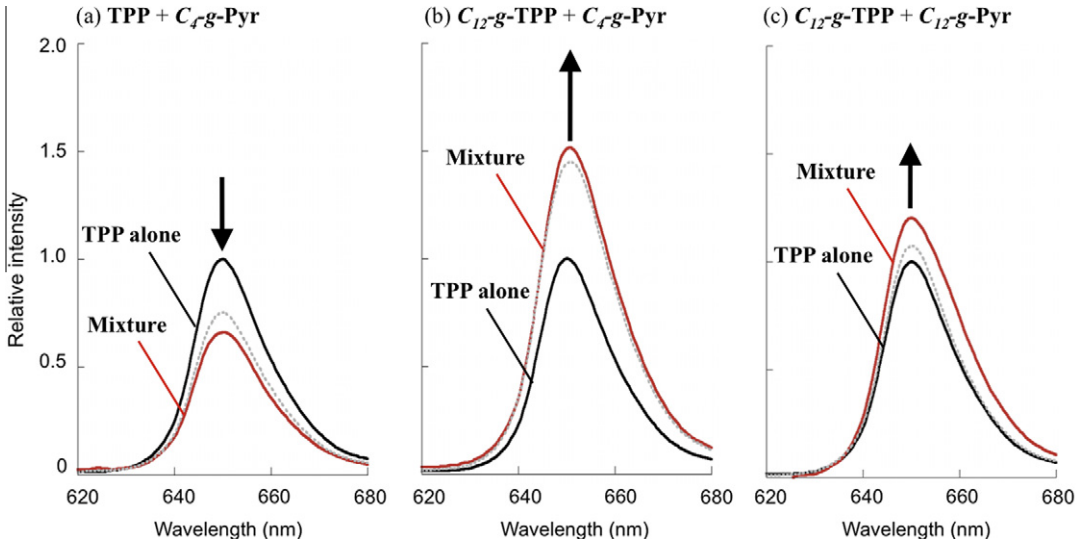

Figure 5. Fluorescence changes in the Q band of ***g*-free TPP** (a) and ***C*$_{12}$-*g*-TPP** (5 μM) with addition of ***C*$_n$-*g*-Pyr** (n = 4 (b) and 12 (c)) in cyclohexane-THF (15:1) at 10 °C. Excitation wavelength: 350 nm.

***C*$_{12}$-*g*-TPP** showed the most effective enhancement of the emission intensity based on the porphyrin moiety when compared with mixed systems of ***C*$_4$-*g*-Pyr** with ***g*-free TPP** and ***C*$_{12}$-*g*-Pyr** with ***C*$_{12}$-*g*-TPP**. These findings indicate that the alkyl chain length not only influences the molecular orientation among pyrene moieties, but also provides a chance to form the preferable molecular fitting for FRET.

Acknowledgment

This work was supported in part by financial support of Japan Society for the Promotion of Science Bilateral Joint Projects.

Supplementary data

Supplementary data (synthesis and characterization of pyrene-derivatives. Experimental detail: TEM measurements, fluorescence and UV–vis spectroscopies) associated with this article can be found, in the online version, at doi:10.1016/j.tetlet.2011.05.131. These data include MOL files and InChiKeys of the most important compounds described in this article.

References and notes

1. McDermott, G.; Prince, S. M.; Freer, A. A.; Hawthornthwaite-Lawless, A. M.; Papiz, M. Z.; Cogdell, R. J.; Isaaca, N. W. *Nature* **1995**, *374*, 517; Roszak, A. W.; Howard, T. D.; Southall, J.; Gardiner, A. T.; Law, C. J.; Isaacs, N. W.; Cogdell, R. J. *Science* **2003**, *302*, 1969; Egawa, A.; Fujiwara, T.; Mizoguchi, T.; Kakitani, Y.; Koyama, Y.; Akutsu, H. *Proc. Natl. Acad. Sci. U.S.A.* **2007**, *104*, 790; Goering, B. K. Ph.D. Dissertation, Cornell University, 1995.
2. Balaban, T. S. *Acc. Chem. Res.* **2005**, *38*, 612; Melkozernov, A. N.; Barber, J.; Blankenship, R. E. *Biochemistry* **2006**, *45*, 331; Huijser, A.; Marek, P. L.; Savenije, T. J.; Siebbeles, L. D. A.; Scherer, T.; Hauschild, R.; Szmytkowski, J.; Kalt, H.; Hahn, H.; Balabvan, T. S. *J. Phys. Chem. C* **2007**, *111*, 11726; Buchanan, J. G.; Sable, H. Z. In *Selective Organic Transformations*; Thyagarajan, B. S., Ed.; Wiley-Interscience: New York, 1972; Vol. 2, pp 1–95.
3. Pasc-Banu, A.; Stan, R.; Blanzat, M.; Perez, E.; Rico-Lattes, I.; Lattes, A.; Labrot, T.; Oda, R. *Colloids Surf., A* **2004**, *242*, 195; Ihara, H.; Takafuji, M.; Sakurai, T. In *Encyclopedia of Nanoscience and Nanotechnology*; Nalwa, H. S., Ed.; American Scientific Publishers: California, CA, 2004; Vol. 9, pp 473–495.
4. Andrews, J. I. M.; Tabor, B. A. *Tetrahedron* **1999**, *55*, 11711.
5. Nakashima, N.; Asakuma, S.; Kim, J.; Kunitake, T. *Chem. Lett.* **1984**, 1709; Ariga, K.; Kikuchi, J.; Naito, M.; Koyama, E.; Norihiro Yamada, N. *Langmuir* **2000**, *16*, 4929.
6. Yamada, K.; Ihara, H.; Ide, T.; Fukumoto, T.; Hirayama, C. *Chem. Lett.* **1984**, *13*, 1713; Ihara, H.; Takafuji, M.; Hirayama, C.; O'Brien, D. F. *Langmuir* **1992**, *8*, 1548.
7. Ihara, H.; Yoshitake, M.; Takafuji, M.; Yamada, T.; Sagawa, T.; Hirayama, C. *Liq. Cryst.* **1999**, *26*, 1021; Ihara, H.; Takafuji, M.; Sakurai, T.; Katsumoto, M.; Ushijima, N.; Shirosaki, T.; Hachisako, H. *Org. Biomol. Chem.* **2003**, *1*, 3004.
8. Li, Y.; Wang, T.; Liu, M. *Soft Matter* **2007**, *3*, 1312; Li, Y.; Liu, M. *Chem. Commun.* **2008**, 5571.
9. Pal, A.; Ghosh, Y. K.; Bhattacharya, S. *Tetrahedron* **2007**, *63*, 7334; Palui, G.; Simon, F. ois-X.; Schmutz, M.; Mesini, P. J.; Banerjee, A. *Tetrahedron* **2008**, *64*, 175.
10. Sagawa, T.; Fukugawa, S.; Yamada, T.; Ihara, H. *Langmuir* **2002**, *18*, 7223.
11. N^2,N^3-Dibutyl-*N*-[4-(1-pyrenylbutyroyl)]-L-glutamide (***C*$_4$-*g*-Pyr**): Triethylamine (0.17 mL, 1.2 mmol) and diethyl-cyanophosphonate (0.17 mL, 1.1 mmol) were added dropwise to the solution of N^2,N^3-dibutyl-L-glutamide (0.22 g, 0.86 mmol) and 1-pyrenylbutylic acid (0.297 g, 1.03 mmol) in chloroform (100 mL) at 0 °C. The reaction solution was stirred for 2 h at 0 °C and then 12 h at room temperature. The mixture solution was washed with aq NaOH solution (0.2 N, 3 × 50 mL), aq. HCl (0.1 N, 3 × 50 mL), and water (50 mL). After the organic layer was dried over Na_2SO_4, the filtrate was concentrated under reduced pressure. The residue was recrystallized from ethanol to yield a desired product as a yellow powder (0.27 g, 58%); mp 213–214 °C; FT-IR (KBr) ν 3290, 3093, 3041, 2957, 2932, 2871, 1637, 1543 cm^{-1}; ^{1}H NMR (400 MHz; $CDCl_3$) δ 0.87–0.91 (6H, m, CH_2CH_3), 1.28–1.35 (4H, m, CH_2CH_3), 1.41–1.50 (4H, m, $NHCH_2CH_2$), 1.90–2.10 (2H, m, CH_2CH_2Ar), 2.19–2.45 (2H, m, CH_2C*H), 2.19–2.26 (2H, m, $C(=O)CH_2(CH_2)_2Ar$), 2.36–2.40 (2H, m, $C(=O)CH_2CH_2C*H$), 3.15–3.36 (4H, m, CH_2NH), 3.37–3.75 (2H, CH_2Ar), 4.34 (1H, q, J = 4.9 Hz, $C*H$), 5.91–5.92 (1H, br, N*H*), 6.77–6.79 (1H, br, N*H*), 7.02–7.04 (1H, br, N*H*), 7.85–8.30 (9H, m, Ar*H*); Anal. Calcd for $C_{33}H_{41}N_3O_3 + 0.5H_2O$: C, 73.85; H, 7.89; N, 7.83. Found: C, 74.11; H, 7.74; N, 7.83.
N^2,N^3-Dioctyl-*N*-[4-(1-pyrenylbutyroyl)]-L-glutamide (***C*$_8$-*g*-Pyr**): diethyl-cyanophosphonate (0.30 mL, 2.0 mmol) were added dropwise to the solution of N^2,N^3-dioctyl-L-glutamide (0.692 g, 1.08 mmol), 1-pyrenylbutylic acid (0.486 g, 1.69 mmol) and triethylamine (0.30 mL, 2.2 mmol) in chloroform (100 mL) at 0 °C. The reaction solution was stirred for 2 h at 0 °C and then 12 h at room temperature. The mixture solution was washed with aq NaOH solution (0.2 N, 3 × 50 mL), aq HCl (0.1 N, 3 × 50 mL), and water (50 mL). After the organic layer was dried over Na_2SO_4, the filtrate was concentrated in vacuo. The residue was recrystallized from ethanol to yield a desired product as a yellow solid powder (0.87 g, 81%): mp 201–202 °C, FT-IR (KBr) ν 3287, 3091, 3040, 2925, 2854, 1637, 1543 cm^{-1}; ^{1}H NMR (400 MHz; $CDCl_3$) δ 0.85–0.89 (6H, q, J = 6.50, CH_3), 1.20–1.26 (10H, br, CH_2CH_3), 1.42–1.49 (4H, m, $NHCH_2CH_2$), 1.91–2.05 (2H, m, $ArCH_2CH_2$), 2.19–2.40 (2H, m, CH_2C*H), 2.18–2.25 (2H, m, $Ar(CH_2)_2CH_2C{=}O$), 2.35–2.40 (2H, m, $C*HCH_2CH_2C{=}O$), 3.15–3.24 (4H, m, $NHCH_2$), 3.35–3.39 (2H, $ArCH_2$), 4.36 (1H, q, J = 6.5 Hz, $C*H$–NH), 5.94–5.96 (1H, br, N*H*), 6.82–6.85 (1H, br, N*H*), 7.03–7.05 (1H, br, N*H*), 7.84–8.29 (9H, m, Ar*H*); Anal. Calcd for $C_{41}H_{57}N_3O_3 + 0.5H_2O$: C, 75.89; H, 9.01; N, 6.48. Found: C, 76.2; H, 8.85; N, 6.52.
12. Ikariya, T., In: *Chemical Society of Japan (Kagakubinran)*, 5th ed.; Iwasawa, Y., Ed.; Maruzen: Tokyo, 2004; Vol. 1, pp 770–777.
13. Terech, P.; Weiss, R. G. *Chem. Rev.* **1997**, *97*, 3133; van Esch, J. H.; Feringa, B. L. *Angew. Chem. Int. Ed.* **2000**, *39*, 2263; Shimizu, T.; Masuda, M.; Minamikawa, H. *Chem. Rev.* **2005**, *105*, 1401; Oda, R. In *Molecular Gels: Materials with Self-Assembled Fibrillar Networks*; Weiss, R. G., Terech, P., Eds.; Springer: Berlin, 2006; pp 577–612.
14. Matile, S.; Berova, N.; Nakanishi, K.; Fleischhauer, J.; Woody, W. R. *J. Am. Chem. Soc.* **1996**, *188*, 5198; Simonyi, M.; Bikádi, Z.; Zsila, F.; Deli, J. *Chirality* **2003**, *15*,

680; Xue, P.; Lu, R.; Li, D.; Jin, M.; Bao, C.; Zhao, Y.; Wang, Z. *Chem. Mater.* **2004**, *16*, 3702.
15. Hatano, M.; Yoneyama, M.; Sato, Y.; Kawamura, Y. *Biopolymers* **1973**, *21*, 2423; Kunitake, T.; Nakashima, N.; Kunitake, M. *Macromolecules* **1989**, *22*, 3544; Sagawa, T.; Tobata, H.; Ihara, H. *Chem. Commun.* **2004**, 2090; Kira, Y.; Okazaki, Y.; Sawada, T.; Takafuji, M.; Ihara, H. *Amino Acids* **2010**, *39*, 587.
16. Takafuji, M.; Ishiodori, A.; Yamada, T.; Sakuraia, T.; Ihara, H. *Chem. Commun.* **2004**, 1122; Liu, X.; Xu, D.; Lu, R.; Li, B.; Qian, C.; Xue, P.; Zhang, X.; Zhou, H. *Chem. Eur. J.* **2011**, *17*, 1660.
17. Kolnig, B.; Pelka, Mario; Zieg, H.; Ritter, T.; Bouas-Laurent, H.; Bonneau, R.; Desvergne, J. *J. Am. Chem. Soc.* **1999**, *121*, 1681; Drovetskaya, T.; Reed, C. A.; Boyd, P. *Tetrahedron Lett.* **1995**, *36*, 7971; Guldi, D. M.; Imahori, H.; Tamaki, K.; Kashiwagi, Y.; Yamada, H.; Sakata, Y.; Fukuzumi, S. *J. Phys. Chem. A* **2004**, *108*, 541.
18. (a) Ishi-i, T.; Iguchi, R.; Snip, E.; Ikeda, M.; Shinkai, S. *Langmuir* **2001**, *17*, 5825; (b) Xiao, Z.; Hou, J.; Jiang, X.; Li, Z.; Ma, Z. *Tetrahedron* **2009**, *65*, 10182; (c) Fukuzumi, S.; Honda, T.; Ohkubo, K.; Kojima, T. *Dalton Trans.* **2009**, 3880; (d) Jintoku, H.; Sagawa, T.; Takafuji, M.; Ihara, H. *Org. Biomol. Chem.* **2009**, *7*, 2430; (e) Gil-Ramírez, G.; Karlen, S. D.; Shundo, A.; Porfyrakis, K.; Ito, Y.; Briggs, G. A. D.; Morton, J. J. L.; Anderson, H. L. *Org. Lett.* **2010**, *12*, 3544.
19. Jintoku, H.; Sagawa, T.; Miyamoto, K.; Takafuji, M.; Ihara, H. *Chem. Commun.* **2010**, 7208.
20. Förster, Th. In *Modern Quantum Chemistry*; Sinanoglu, O., Ed.; Academic Press: New York, 1965; p 93; Sapsford, K. E.; Berti, L.; Medintz, L. *Angew. Chem. Int. Ed.* **2006**, *45*, 4562.